Neurological Sciences (2019) 40:339–349
https://doi.org/10.1007/s10072-018-3638-1

ORIGINAL ARTICLE

Disturbed effective connectivity patterns in an intrinsic triple network model are associated with posttraumatic stress disorder

Yifei Weng[1] · Rongfeng Qi[1] · Li Zhang[2] · Yifeng Luo[3] · Jun Ke[1] · Qiang Xu[1] · Yuan Zhong[1] · Jianjun Li[4] · Feng Chen[4] · Zhihong Cao[3] · Guangming Lu[1]

Received: 19 June 2018 / Accepted: 7 November 2018 / Published online: 17 November 2018

Abstract

Background Disturbance of the triple network model was recently proposed to be associated with the occurrence of posttraumatic stress disorder (PTSD) symptoms. Based on resting-state dynamic causal modeling (rs-DCM) analysis, we investigated the neurobiological model at a neuronal level along with potential neuroimaging biomarkers for identifying individuals with PTSD.

Methods We recruited survivors of a devastating typhoon including 27 PTSD patients, 33 trauma-exposed controls (TECs), and 30 healthy controls without trauma exposure. All subjects underwent resting-state functional magnetic resonance imaging. Independent components analysis was used to identify triple networks. Detailed effective connectivity patterns were estimated by rs-DCM analysis. Spearman correlation analysis was performed on aberrant DCM parameters with clinical assessment results relevant to PTSD diagnosis. We also carried out step-wise binary logistic regression and receiver operating characteristic curve (ROC) analysis to confirm the capacity of altered effective connectivity parameters to distinguish PTSD patients.

Results Within the executive control network, enhanced positive connectivity from the left posterior parietal cortex to the left dorsolateral prefrontal cortex was correlated with intrusion symptoms and showed good performance (area under the receiver operating characteristic curve = 0.879) in detecting PTSD patients. In the salience network, we observed a decreased causal flow from the right amygdala to the right insula and a lower transit value for the right amygdala in PTSD patients relative to TECs.

Conclusion Altered effective connectivity patterns in the triple network may reflect the occurrence of PTSD symptoms, providing a potential biomarker for detecting patients. Our findings shed new insight into the neural pathophysiology of PTSD.

Keywords Posttraumatic stress disorder · Resting-state fMRI · Dynamic causal modeling · Triple network model

Yifei Weng, Rongfeng Qi and Li Zhang contributed equally to this work.

Electronic supplementary material The online version of this article (https://doi.org/10.1007/s10072-018-3638-1) contains supplementary material, which is available to authorized users.

✉ Feng Chen
fenger0802@163.com

✉ Zhihong Cao
staff877@yxph.com

✉ Guangming Lu
cjr.luguangming@vip.163.com

[1] Department of Medical Imaging, Jinling Hospital, Medical School of Nanjing University, 305 Zhongshan East Road, Xuanwu District, Nanjing 210002, Jiangsu Province, China

[2] Mental Health Institute, the Second Xiangya Hospital, National Technology Institute of Psychiatry, Key Laboratory of Psychiatry and Mental Health of Hunan Province, Central South University, No.139 Middle Renmin Road, Changsha 410011, Hunan Province, China

[3] Department of Radiology, The Affiliated Yixing Hospital of Jiangsu University, 75 Tongzhenguan Road, Wuxi 214200, Jiangsu Province, China

[4] Department of Radiology, Hainan General Hospital, Haikou 570311, China

Introduction

Posttraumatic stress disorder (PTSD) is the most common psychiatric consequence of experiencing severe traumatic events and is characterized by a set of symptoms including intrusive thoughts, avoidance, and hyper-vigilance [1] along with clinical manifestations such as sleep disturbance and emotional and cognitive disorders [2]. These recurrent and intractable symptoms severely affect the quality of life of individuals with PTSD. The current diagnostic criteria for PTSD highlight the role of negative cognition in patient evaluation and treatment [3]. For therapeutic strategies to be successful, careful clinical assessment that can detect changes in the cognitive network of PTSD patients is needed [4]. Elucidating causal relationships in biological triple network models related to cognition could improve diagnosis and provide preliminary neuroimaging biomarkers for PTSD.

The concept of "triple model," which brought forward by Menon [5], includes the default mode network (DMN), executive control network (ECN), and salience network (SN). All the three networks could be readily identified under different cognitive tasks, and their response increase and decrease in proportion, and often interact antagonistically. The inappropriate assignment of the three networks to external tasks or internal events would lead to neural pathological status [5, 6]. A battery of researches has proved that the triple network model provided a reliable framework to detect the altered cognitive and affective function in a wide range of psychiatric and neurological conditions including PTSD [7–12]. The DMN, which controls internal thought and autobiographical memory, is hypoactive in PTSD patients during the resting state and is triggered when they are engaged in a task [13, 14]. Most cognitive processing paradigms associated with the ECN exhibit network deactivation [15, 16], with the dorsolateral prefrontal cortex (dlPFC) serving as a critical hub in the network that shows increased activity in fMRI studies [17]. As for the SN, the amygdala—a dispensable hub linked to PTSD pathology—usually shows excessive activation and enhanced inter-regional connectivity with the insula [9, 18], whereas findings in the dorsal anterior cingulate cortex (dACC) were more flexible [18–20]. Studies investigating interactions across the three networks have demonstrated that increased communication between the DMN and SN may underlie the occurrence of hyper-vigilance and intrusive symptoms in PTSD [9, 21]. Interestingly, the traditional neural circuit emphasizes the decreased inhibition of medial prefrontal cortex (mPFC), with disabled top-down control over the limbic areas including the amygdala and hippocampus, which are also the critical nodes of the triple network model [12]. Accordingly, the two different neural models should be taken into consideration when investigating the neuropathophysiology underlying PTSD, while the triple network model could provide a better understanding of the cognitive involvement.

Most previous fMRI studies have focused on indirect regional activation—i.e., amplitude of low-frequency fluctuation [22] and regional homogeneity [23]—or inter-regional time series synchronization—i.e., seed-based functional connectivity [10]. Routine functional connectivity analyses cannot reveal underlying hierarchical organization of connectivity or distinguish the direction of coupling between regions [24]. Resting-state dynamic connectivity modeling (rs-DCM) is a novel algorithm for constructing a plausible neuronal model of coupled neuronal states and generating complex cross-spectra among responses to measure directed neural influences [25]. This method provides a straightforward and efficient means of estimating direct neural coupling and vascular parameters and hidden neuronal fluctuations in PTSD patients, which could partly overcome the limitations of conventional data analysis.

In the current study, we carried out an rs-DCM analysis of DMN, ECN, and SN effective connectivity patterns in PTSD patients in order to identify changes in the triple network model, which could yield new insight into the neural pathophysiology of PTSD.

Material and methods

Subjects

An estimated 9–57% of individuals have experienced PTSD following natural disasters in Asia [26]. In July 2014, Typhoon Rammasun, one of only two Category 5 super typhoons recorded since 1954, struck Wenchang City near the South China Sea. The devastating storm caused at least 14 deaths, and more than 1000 people were trapped and nearly drowned. All of the residents suffered from enormous grief and losses. We recruited 70 typhoon-exposed subjects from this area 3 months later. Each survivor was screened with the PTSD Checklist–Civilian Version (PCL_C) [27]. Those who scored over 35 were evaluated with the Clinician-Administered PTSD Scale (CAPS) [28]; those scoring < 30 were designated as trauma-exposed controls (TECs). The CAPS for the Diagnostic and Statistical Manual of Mental Disorders, 4th edition (DSM-IV) consists of a structured interview to assess the frequency and intensity of each PTSD symptom. Comorbidity was determined with the DSM-IV Structured Clinical Interview [29]. To evaluate working memory and visual memory dysfunction in PTSD patients, we used the subtests of the Wechsler Memory Scale for logical memory and visual reproduction [30]. We also recruited 30 age- and gender-matched healthy controls (HCs) that did not meet DSM-IV criteria for any psychiatric condition. Before MRI scanning, all participants were assessed with the Self-Rating Anxiety Scale (SAS) [31] and Self-Rating Depression Scale (SDS) [32] to evaluate anxiety and depression symptoms. The

local medical research ethics committee approved this prospective study and written, informed consent was obtained from each participant.

Exclusion criteria for participants were (1) age < 18 years or > 65 years, (2) left-handedness, (3) history of head injury or loss of consciousness, (4) significant medical or neurological conditions, (5) lifelong or current psychiatric disorders other than depression or anxiety, (6) substance abuse, (7) contraindication for MRI, and (8) > 1.5 mm maximum displacement in translation or 1.5° rotation in any direction.

Data acquisition and preprocessing

Rs-fMRI images were acquired on a 3.0-Tesla MR scanner (Skyra; Siemens Medical Solutions, Erlangen, Germany) with a standard head coil at the People's Hospital of Hainan Province. During data acquisition, participants were instructed to lay supine and remain still in the scanner with their eyes closed without falling asleep. The subjects' head was immobilized with padding and earplugs were provided to improve noise tolerance during the scan. The blood oxygenation level-dependent fMRI dataset was collected by performing an echo-planar imaging sequence with the following parameters: repetition time (TR), 2000 ms; echo time (TE), 30 ms; flip angle, 90°; field of view (FOV), 230 × 230 mm^2; 250 volumes; and matrix, 64 × 64; slice thickness, 3.6 mm; no intersection gap; the total acquisition time, 508 s. Each volume included 35 axial slices for whole-brain coverage aligned along the anterior–posterior commissure line. High-resolution T1 structural images in the sagittal orientation were acquired using a rapid gradient-echo sequence with the following parameters: TR, 2300 ms; TE, 1.97 ms; flip angle, 9°; FOV, 256 × 256 mm^2; 176 slices; slice thickness, 1 mm; the total acquisition time, 353 s. The routine T1-weighted and T2 fluid-attenuated inversion recovery images were obtained for each subject for conventional diagnosis and were reviewed by two experienced radiologists to exclude any structural lesions.

The rs-fMRI data were preprocessed using Data Processing Assistant for Resting-State fMRI Advanced Edition (http://www.restfmri.net) based on the MATLAB platform (Math Works, Natick, MA, USA) [33]. The first 10 time points were removed for signal equilibrium. After slice timing, realignment, and spatial normalization, the remaining 240 volumes were co-registered with corresponding T1 anatomical images, which were segmented and warped into Montreal Neurological Institute (MNI) space with a final isotropic size resolution of 3 mm. The pipeline also spatially smoothed the data using a Gaussian kernel of 8 mm full width at half maximum.

Selection of regions of interest (ROIs)

Spatial independent component analysis (ICA) was performed to identify the ROIs within the DMN, ECN, and SN using Group ICA of fMRI Toolbox (GIFT, http://mialab.mrn.org/software/gift) [34]. We delineated 31 components from the data of all 90 subjects. To reduce data dimensions, principal component analysis was performed as a preprocessing step. Single subject time courses and spatial maps were back-reconstructed. The resultant components of the ICA were those most closely correlated spatially with pre-existing RSN templates of the GIFT toolbox. For our DCM analysis, ROIs were identified from the best-matching independent components of DMN, ECN, and SN based on one-sample *t* test maps at each group level [35].

According to the results of group ICA, three independent components were selected by spatially maximal matching to pre-existing DMN, ECN, and SN templates. The DMN included four nodes: mPFC, posterior cingulate cortex (PCC)/precuneus, and right and left angular gyri. The ECN comprised of four nodes: right and left dorsolateral prefrontal cortex (dlPFC) and bilateral posterior parietal cortex (PPC). The SN contains five nodes: dACC, right and left insula, and bilateral amygdala (Fig. 1).

Spectral dynamic connectivity modeling analysis

After selecting seed regions, we performed a general linear model (GLM) analysis to extract ROI-specific time series from original preprocessed data for DCM analysis. We computed the principal eigenvalue of a sphere with an 8-mm radius centered at the coordinates of the peak *t* value of each ROI in each group based on the aforementioned one-sample *t* test results. For the inter-network analysis, we extracted a time series from subject-specific ICA time courses for each network [36]. The GLM also included mean signals for six rigid body realignment parameters with white matter and cerebrospinal fluid as regressors. We then constructed dynamic causal models of the three networks with the identified ROIs using the DCM12 routine in SPM12 (Wellcome Department of Cognitive Neurology, London, UK; www.fil.ion.ucl.ac.uk/spm). For each participant, the average effective connectivity between regions during resting-state analysis was modeled by second-order statistics (complex cross-spectra) to characterize spectral density over various frequencies. The spectral DCM is an extension of DCM that employs the Fourier transform of the cross-correlation rather than direct computation of time series as a data feature for prediction. The models reveal hidden neuronal and biophysical states that generate data and yield a predicted blood oxygen level-dependent contrast imaging signal. Post hoc model optimization [37] was applied to determine the best-fitting model for the data. We constructed a fully connected model without exogenous inputs and used the Bayesian model reduction procedure to test every possible model nested in the full model. This method, which yields results similar to Bayesian model selection, considered all possible generated models by removing all permutations of

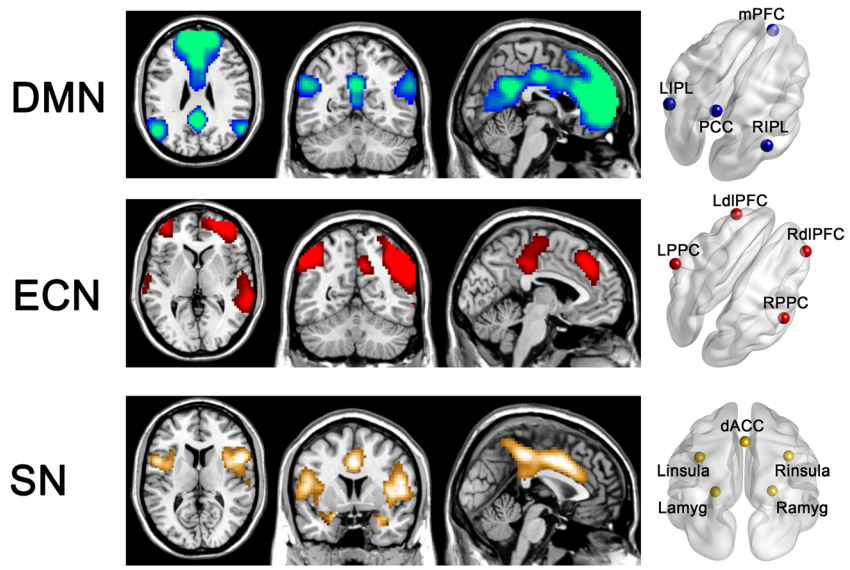

Fig. 1 Defined ROI with spatial independent component analysis. Spatial maps of DMN, ECN, and SN at group level are identified with ICA. Using the xjview and BrainNet Viewer, the schematic mapping and nodes distribution are shown

the parameters of each model whose individual removal led to the smallest reduction in model evidence [38]. The model exhibiting the highest probability was ultimately selected. This post hoc procedure yields a valid estimation of the model evidence and requires less computational time.

Statistical analysis

SPSS v.22.0 (SPSS Inc., Chicago, IL, USA) was used to analyze demographic and clinical data. The SPM 8 statistical software (FIL Methods Group; http://www.fil.ion.ucl.ac.uk/spm/doc/biblio/) was used to create one-sample *t* test maps of the three target networks at the group level for all subjects (statistical maps were corrected to $P < 0.05$ using family-wise error rate).

Based on spectral DCM analysis, connectivity strength [39] (DCM. Ep. A) differing significantly from zero showing a strong connection was revealed by the random effects one-sample t test. We depicted the connectivity patterns of each model to identify significant effective connectivities ($P < 0.05$) and then performed analysis of covariance with educational level as well as depression and anxiety scores as covariates to evaluate differences in effective connectivity strength, neural amplitude, and exponents (DCM. Ep. a) and hemodynamic parameters (e.g., transit and decay) across the three groups [39] Post hoc tests were applied to the significant results ($P < 0.05$, Bonferroni corrected).

To investigate the association between clinical manifestations of PTSD and brain activity, we separately performed a Spearman correlation analysis of PCL_C scores, CAPS total and sub-symptomology scores, logical memory and visual reproduction scores, and SAS and SDS scores with all effective connectivity parameters in each group using SPSS software, with significance set at $P < 0.05$.

Receiver operating characteristic (ROC) curve analysis

The binary logistic regression was used to determine the contribution of altered effective connectivity parameters to PTSD outcome and whether the aberrances act as the risk factors. In order to reserve the eligible indices information ($P < 0.05$) and advance the final model, we adopt the step-wise regression and estimated the prediction probability of the eligible indices. Consequently, the ROC analysis was carried out to examine whether the altered effective connectivity parameters could serve as the potential biomarker for distinguishing PTSD patients from TEC and HC cohorts. The area under the curve (AUC) was assessed using the SPSS software, and the corresponding optimal cut-off value was determined by maximizing Youden's index *J* (J = sensitivity + specificity − 1).

Results

Demographic and clinical data

After excluding 1 patient with brain infarction, 1 with pregnancy and 8 with ineligible imaging data, we ultimately enrolled 27 PTSD patients, 33 TECs, and 30 HC in this study. Demographic and clinical data for all study subjects are summarized in Table 1. There were no significant differences among the three groups in terms of gender ($P = 0.912$) or age ($P = 0.729$). However, education level was higher in HCs than in the other two groups ($P < 0.001$), whereas PCL_C scores were higher in the PTSD group than in TECs ($P < 0.001$). The PTSD group had a mean CAPS total score of 78.18 ± 19.29, and sub-scale scores of symptom clusters (intrusive thoughts, avoidance, and hyper-vigilance) were 25.52 ± 7.27, 28.07 ± 8.26, and 25.59 ± 6.92, respectively. These patients performed poorly on the logical memory and

Table 1 Summary of demographic and clinical data

	PTSD ($n = 27$)	TEC ($n = 33$)	HC($n = 30$)	P value
M to F ratio	7:20	7:26	7:23	0.912[a]
Age (year)	48.41 ± 10.32	48.45 ± 7.48	49.87 ± 6.11	0.729[b]
Education (year)	6.41 ± 3.35	6.97 ± 3.36	9.73 ± 3.29	< 0.001[b]
SAS score	52.63 ± 10.63	33.09 ± 6.60	28.77 ± 4.38	< 0.001[b]
SDS score	55.67 ± 10.56	33.06 ± 7.38	26.83 ± 5.72	< 0.001[b]
PCL_ C score	53.74 ± 8.46	28.94 ± 5.44		< 0.001[c]
Logical memory	2.84 ± 2.99		8.03 ± 3.49	< 0.001[d]
Visual reproduction	4.92 ± 3.60		9.47 ± 2.62	< 0.001[d]
CAPS total score	78.18 ± 19.29			
Intrusion	24.52 ± 7.27			
Avoidance	28.07 ± 8.26			
Hyper-vigilance	25.59 ± 6.92			

Data are means ± standard deviations

PTSD posttraumatic stress disorder, *TEC* traumatic exposed controls, *HC* healthy controls, *M* male, *F* female, *PCL* PTSD Checklist–Civilian Version, *CAPS* Clinical-Administered PTSD Scale, *SAS* Self-Rating Anxiety Scale, *SDS* Self-Rating Depression Scale

[a] *P* value calculated with chi-square test

[b] *P* value calculated with one-way analysis of variance

[c] *P* value calculated with two-sample *t* test

[d] *P* value calculated with Mann-Whitney *U* test

visual reproduction tasks, and two subjects failed to finish all the tasks. We also observed that the three groups had significantly different SAS and SDS scores ($P < 0.001$) in the rank order of PTSD > TEC > HC.

Spectral dynamic causal modeling analysis

The detailed information of ROI coordinates for DCM analysis is shown in Table 2. A search of the model space by post hoc model optimization revealed that the fully connected model with a posterior probability of almost 1 and log probability of almost 0 was the most plausible model for each group. The profile of model evidence with the posterior probability is shown in Appendix Figure 1. The strength and direction of each connection within each model were evaluated (Fig. 2; detailed parameters are shown in Appendix Table 1). The fully connected DMN, ECN, SN, and between network models contained 16, 16, 25, and 9 parameters, respectively, describing the effective connectivity strength (self-connections were excluded from our final results for simplicity). In the DMN, HCs showed symmetrical effective connectivity from the mPFC and PCC to bilateral angular gyri and a strong effective interaction between bilateral angular gyri. However, PTSD patients and the TEC group showed decreased effective connectivity strength from the mPFC to the left angular gyrus. For the ECN, we found an increased effective connectivity from the left PPC to the left dlPFC in

Table 2 Peak voxel coordinates of the major nodes for DCM analysis

Brain region	Peak voxel MNI coordinate (x, y, z)		
	PTSD	TEC	HC
DMN			
mPFC	6, 60, 27	3, − 51, 24	− 3, 48, 6
PCC	− 1, − 54, 27	− 3, − 48, 30	− 1, − 48, 33
R_angular	57, − 63, 30	54, − 63, 30	54, − 63, 27
L_angular	− 48, − 69, 33	− 51, − 66, 36	− 51, − 63, 30
ECN			
R_dlPFC	39, 51, − 3	33, 54, − 3	42, 51, − 9
L_dlPFC	− 39, 54, − 3	− 42, 54, 0	− 42, 48, − 9
R_PPC	48, − 48, 48	45, − 57, 48	45, − 48, 48
L_PPC	− 48, − 51, 54	− 42, − 63, 51	− 48, − 69, 36
SN			
R_amygdala	21, 0, − 12	23, − 4, − 12	21, − 3, − 15
L_amygdala	− 21, 0, − 12	− 18, − 6, − 15	− 21, 0, − 18
dACC	1, 26, 33	0, 21, 36	6, 18, 42
R_insula	39, 18, 3	36, 18, 9	33, 18, 6
L_insula	− 39, 15, 0	− 42, 15, 6	− 42, 15, 6

MNI Montreal Neurological Institute, *PTSD* posttraumatic stress disorder, *TEC* traumatic exposed controls, *HC* healthy controls, *DMN* default mode network, *ECN* executive control network, *SN* salience network, *mPFC* medial prefrontal cortex, *PCC* posterior cingulate cortex, *dlPCF* dorsolateral prefrontal cortex, *PPC* posterior parietal cortex, *dACC* dorsal anterior cingulate cortex, *R* right, *L* left

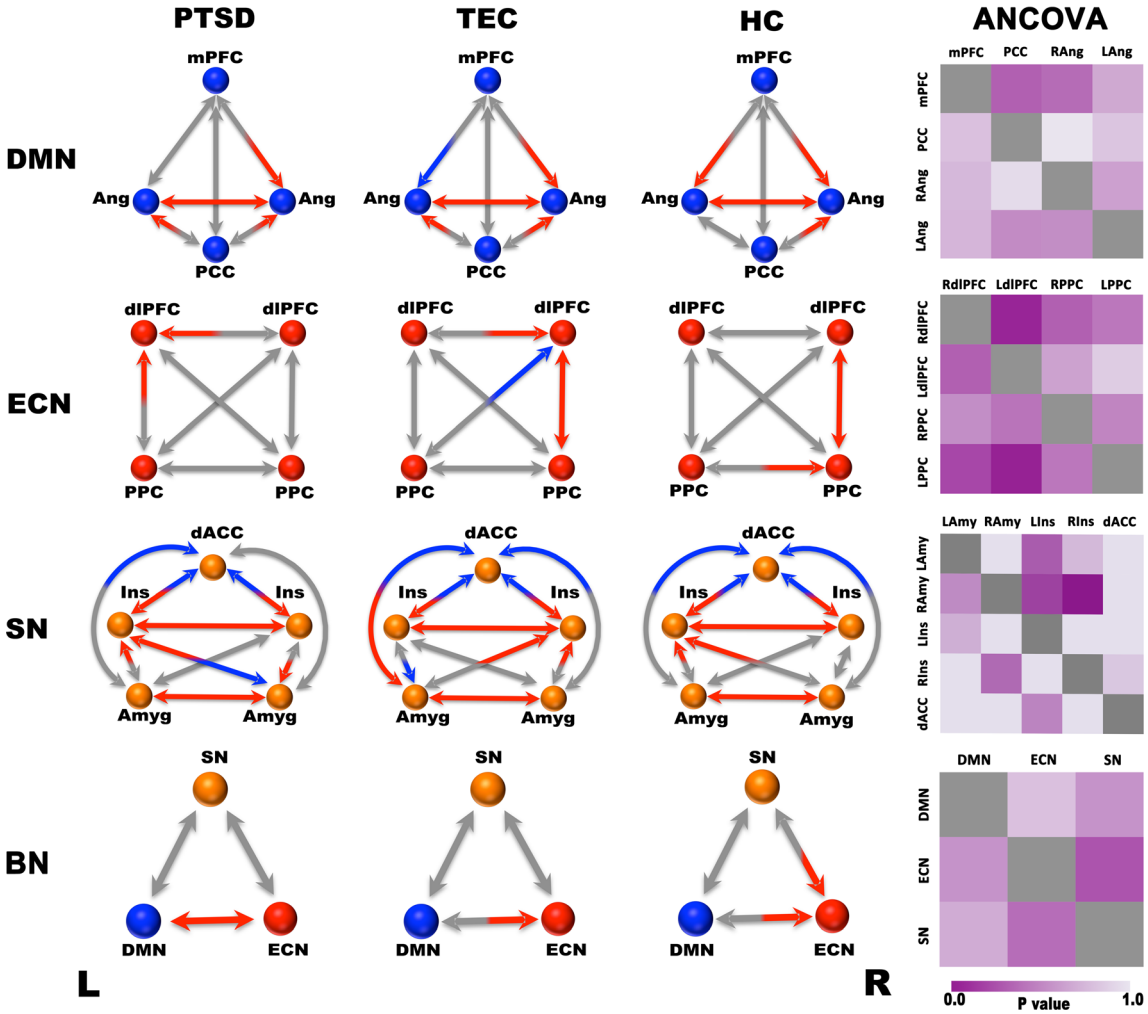

Fig. 2 Effective connectivity patterns of intra- and inter-networks in each group and color matrix of ANOVA result among groups. The robust effective connectivity is displayed with coloring arrows. Arrows in red means significantly positive different from 0 and arrows in blue are significantly negative different from 0. The *P* values of the analysis of variances test are shown with color matrix, and the connections with significant differences are demonstrated with deeper color. The vertical columns represented the source region and the horizontal rows indicated the target region for the connectivity parameters The differences among groups are obviously observed from left dlPFC to left PPC in ECN and right amygdala to right insula in SN

the PTSD group, as well as an absence of effective flow between the right dlPFC and right PPC. Additionally, altered effective connectivity patterns between bilateral dlPFC, bilateral PPC, and left PPC to right dlPFC were observed in the PTSD and TEC groups. In the SN, we observed symmetrical effective connectivity patterns of dACC along with interactional effective connectivity between bilateral insula and the amygdala in the HC group. Notable changes in the PTSD group were the effective connectivity of the right amygdala with other SN regions including left insula, right insula, and dACC, while the TEC group exhibited altered effective connectivity patterns in the interaction between bilateral amygdala and insula. Between networks, all the groups showed positive effective connectivity from DMN to ECN. The PTSD groups had increased effective connectivity from ECN to DMN. Moreover, the effective connectivity from SN to ECN, which could be detected in HC group, was absence in TEC and HC group.

In the post hoc analysis, we found an increased positive connectivity from the left PPC to the left dlPFC within the ECN in both the TEC and PTSD groups, whereas PTSD patients showed significant enhancement relative to HCs. Within the SN, we found decreased causal flow from the right amygdala to the right insula in PTSD patients relative to TEC group ($P < 0.05$, Bonferroni corrected for multiple comparisons). Although our analysis failed to detect significant inter-group differences in the DMN and between networks, there were nonetheless some alterations in effective connectivity. We also observed that the transit values of the right amygdala—one of the hemodynamic parameters—were significantly decreased in PTSD patients (Table 3 and Fig. 3). To simplify our result, all neural

Table 3 Effective connectivity parameters differences across three groups

Brain region	*F* score	Sig.			*P* value
PTSD vs. TEC			PTSD	TEC	
			Strength	Strength	
R_amygdala to R_insula	3.759	0.027	− 0.2383 ± 0.7810	0.3536 ± 0.8514	0.029
			Transit value	Transit value	
R_amygdala	3.674	0.029	− 0.4762 ± 0.2196	− 0.3062 ± 0.2582	0.032
PTSD vs. HC			PTSD	HC	
			Strength	Strength	
L_PPC to L_dlPFC	3.955	0.023	0.5230 ± 0.5328	0.0532 ± 0.7726	0.023

Significant effective connectivity at the group level ($P < 0.05$, Bonferroni corrected)

PTSD posttraumatic stress disorder, TEC traumatic exposed controls, *HC* healthy controls, *Sig.* significance, *R* right, *L* left, *PPC* posterior parietal cortex, *dlPFC* dorsolateral prefrontal cortex

and hemodynamic parameters were displayed in Appendix Figure 2.

Correlation results

We observed a positive correlation between CAPS sub-scale scores of intrusion symptoms and mean effective strength from the left PPC to the left dlPFC ($r = 0.401$, $P < 0.05$) (Fig. 4a).

ROC results

The altered effective connectivity strength from left PPC to left dlPFC acts as a risk factor contributed to PTSD outcome, while the other altered parameters did not show their contributions to the model (detailed result of binary logistic regression was reported in Appendix Table 2). Additionally, the ROC result showed a good performance for distinguishing

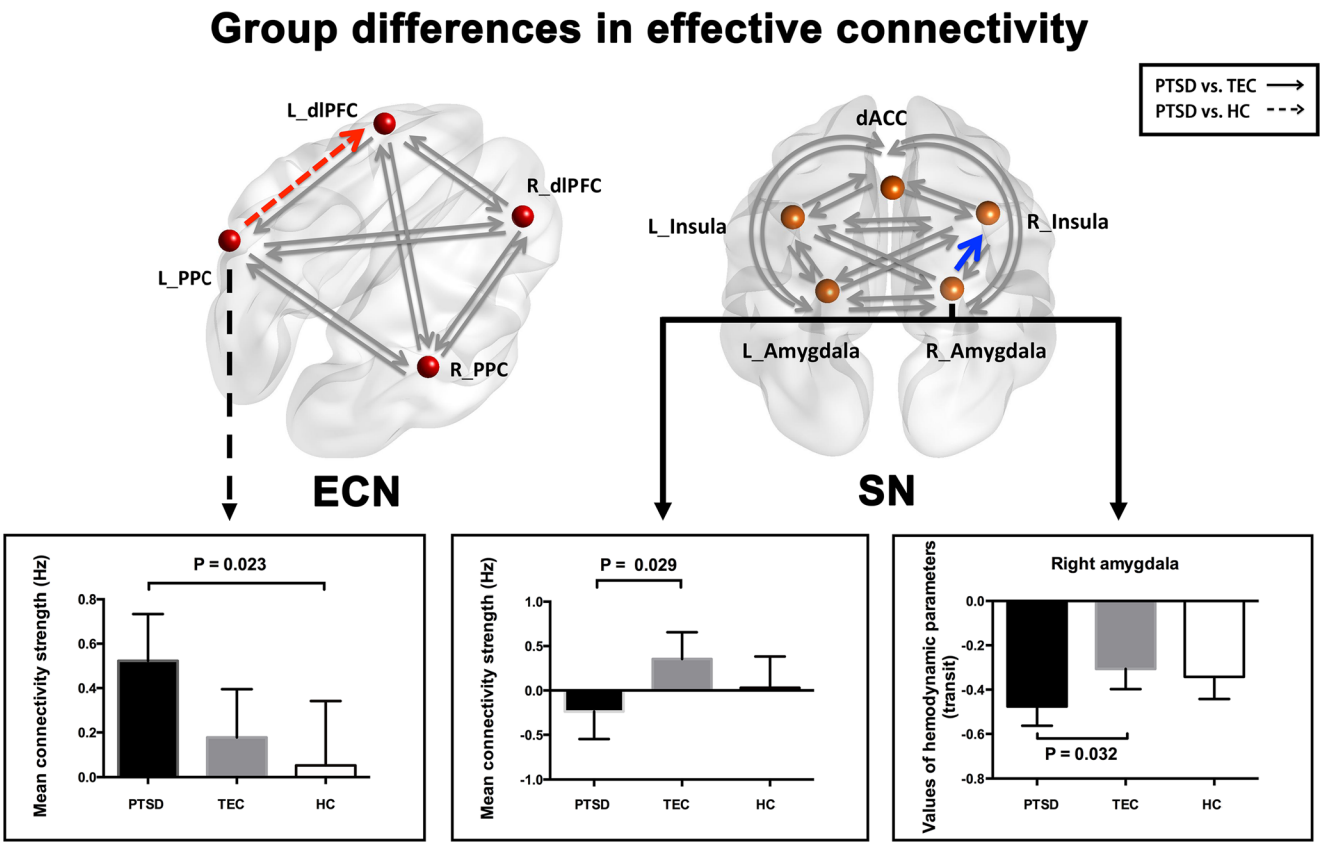

Fig. 3 Significant differences in effective parameters estimated between groups. Within ECN, significantly increased effective connectivity strength from left posterior parietal cortex to left dorsolateral prefrontal cortex (red dashed arrow) is found in PTSD patients relative to healthy controls. Within SN, PTSD patients exhibit relatively decreased effective connectivity from right amygdala to right insula (blue solid arrow) and lower transit value of right amygdala compared with TEC group. The detailed altered effective connectivity parameters display in the form of bar chart. *Significant different ($P < 0.05$); error bar, 95% confidence interval (CI)

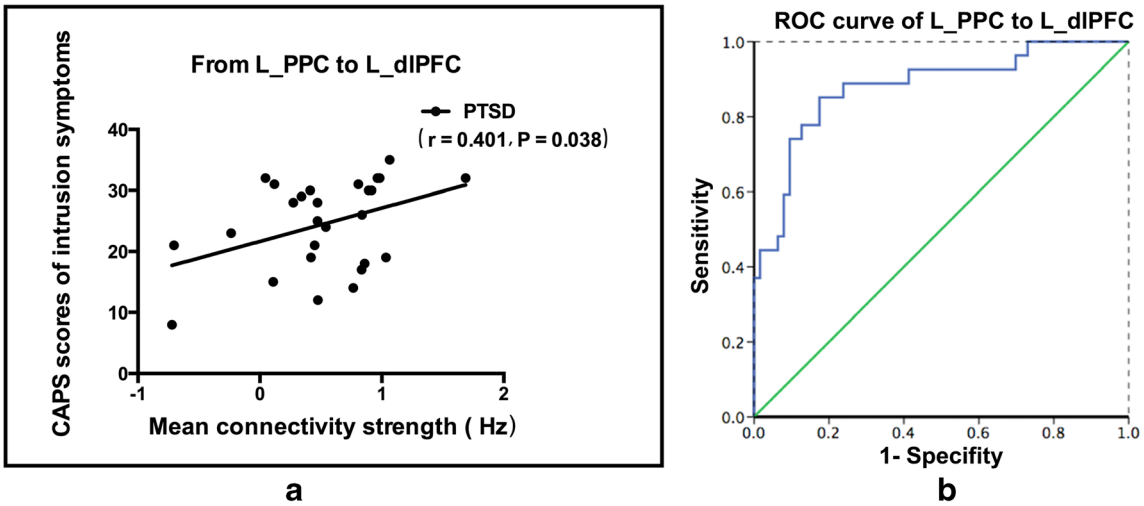

Fig. 4 Significant correlation between intrusion symptom of PTSD patients and effective connectivity strength and ROC analysis from left PPC to left dlPFC. **a** CAPS sub-symptom scores of intrusion positively correlate with the effective connectivity strength from left posterior parietal cortex to left dorsolateral prefrontal cortex. **b** ROC analysis for detecting PTSD patients from non-PTSD subjects

PTSD patients from non-PTSD subjects (AUC = 0.879, cut-off value 0.108), with a sensitivity of 85.2% and specificity of 82.5% (Fig. 4b).

Discussion

The results of this study demonstrated that PTSD patients have disrupted effective connectivity patterns mainly in the ECN and SN. ECN abnormalities were correlated with clinical symptoms in PTSD patients. The rs-DCM analysis revealed that altered endogenous causal flow within the intrinsic triple network model plays an important role in the psychopathology of PTSD.

Rs-DCM analysis is a new deterministic approach that offers an efficient way of assessing the causal relationships between specific brain regions by identifying not only reciprocally effective connectivity but also neuronally and hemodynamically active status [25]. Compared to other effective connectivity measurement methods such as structural equation modeling [40] and Granger causality analysis [41], DCM provides a more precise estimation of a fMRI times series and explicitly models the neuronal basis of the rate of change of hemodynamic response underlying effective connectivity [25]. Thus, rs-DCM is more informative for drawing inferences about causal links within brain networks.

The DMN effective connectivity patterns in PTSD patients

Although we did not note any obvious changes within the DMN, the effective connectivity from the mPFC to the left angular gyrus showed a decreasing trend, suggesting a tendency of intrinsic DMN instability in PTSD patients. Many fMRI studies have confirmed the decreased connectivity between DMN nodes in PTSD patients as compared to TECs and HCs [10]. However, the rs-DCM analysis is not sufficiently sensitive to detect obvious changes within the DMN, which must be analyzed using other fMRI techniques.

The altered ECN effective connectivity patterns in PTSD patients

We observed increased resting-state effective connectivity from the PPC to dlPFC within the ECN in PTSD patients. A recent study reported enhanced inter-regional connectivity between left dlPFC and left PPC [42], which is in accordance with our findings. This provides new evidence that endogenous connectivity enhancement in PTSD results from increased causal flow between these two brain regions. The PPC receives information input from the visual, auditory, and somatic sensory systems, which contribute to spatial reasoning, movement planning, and attention [43]. Most outputs to the frontal motor cortex—which includes the dlPFC, the most critical node of the ECN—shows increased activity in PTSD patients in cognitive paradigms [44, 45]. Meanwhile, the dlPFC and PPC are essential hubs of the frontoparietal attention network [46]. It was demonstrated that increased functional connectivity between the dlPFC and parietal cortex was associated with severity of PTSD symptoms [47]. Damage to the top-down attentional control circuit disrupts the assignment of attention resources to internal or external stimuli, which in turn contributes to symptoms such as dissociative reactions (e.g., flashbacks) or intense or prolonged psychological distress when PTSD patients are exposed to cues that

resemble aspects of the traumatic event [2]. This was supported by our finding of a positive correlation between CAPS sub-scores of intrusion symptoms and the effective connectivity strength from the left PPC to the left dlPFC. Moreover, the good performance of the ROC curve suggested that the enhanced effective connectivity from the PPC to the dlPFC can presumably detect aberrant neural activity in PTSD patients with high specificity and sensitivity.

The altered SN effective connectivity patterns in PTSD patients

The amygdala is considered as a critical hub of the salience network [48]. An altered effective connectivity from the right amygdala to the right insula was observed in PTSD patients. More specifically, the type of causal flow changed from positive to negative. Impaired structural and functional integrity in the SN has been proposed as a transdiagnostic feature of a broad spectrum of psychiatric illnesses [49]. With regard to PTSD, it has been suggested that disturbed functional interactions within the SN are responsible for hyper-vigilance and emotional disturbance [19]. A recent [^{18}F]-FDG positron emission tomography animal study revealed that disruption of the causal link in the prefronto-amygdala-insula pathway might alter metabolic activity within the amygdala and insula under fear-inducing conditions [50]. It has been suggested that the aberrant filtering and mapping of salient stimulus into the SN would lead to signal deficits, especially between insula and the amygdala, which also observed in our study. This abnormality was also responsible for the cognitive and affective dysfunction in other neurological and psychiatric diseases [5]. Meanwhile, we also found declining transit values in the right amygdala of PTSD patients, representing a shortened passage time of a blood cell through the capillary bed, which could affect metabolic activity [25, 51]. Thus, the results of the current study combined with previous reports indicate that excessive neural activity in the amygdala contributes to exaggerated fear response and persistent traumatic memories in PTSD patients [10].

The inter-network effective connectivity patterns in PTSD patients

In current study, the effective connectivity from the ECN to the DMN gyrus showed a tendency of increase in PTSD patients, though we fail to detected significant group differences. In our recent published literature [52], we have reported that left ECN in PTSD group predicted subsequent increased activity of posterior DMN, which has demonstrated the specific effective connectivity alteration within the triple network model. It should be noted that the trend of unbalance from SN to ECN could also be observed in PTSD group. The triple network model highlights the role of SN in initiating network switching of the CEN engagement and DMN disengagement [5]. The weakened signaling transmission from SN to ECN in PTSD patients might disturb the process of cognitive event triggering.

Limitations

This study had some limitations. Firstly, it should be considered as a pilot study given the modest sample size. Secondly, the educational level of the PTSD and TEC groups was lower than that of HCs. In order to minimize the influence of this difference, we screened all participants with the Mini-Mental State Examination to exclude the mental retardation, and statistical analysis of fMRI data was performed using educational level as a covariate. Additionally, we administered only two subtests of the Wechsler Memory Scale to detect the cognitive disorders in PTSD, since redundant testing could discourage participant cooperation. Lastly, cross-network interactions require further dynamic observation to clarify the mechanisms underlying the triple network model.

Conclusion

The results presented here demonstrated the disturbed effective connectivity patterns of the intrinsic triple network model in PTSD patients. Specifically, we uncovered aberrant causal connectivity in the ECN and SN and identified altered effective connectivity from the left PPC to the left dlPFC as a probable biomarker for distinguishing PTSD patients. These findings provide new insight into the neural substrates of PTSD.

Author contributions YW was involved in the experimental design, data analysis, and writing of the manuscript. RQ, ZC, FC, and GL designed the study. JK, QX, and YZ analyzed the data. YL, JL, and LZ acquired the data.

Funding This work was supported by the grants from the National Nature Science Foundation of China [Grant Numbers 81671672, 81301209, 81301155, 81460261, and 81201077]; the Key Science and Technology Project of Hainan Province [grant number ZDYF2016156]; and the Chinese Key Grant [Grant Number BWS11J063]; Jiangsu Provincial Medical Youth Talent [grant number QNRC2016888]; Foundations of Commission of Health and Family Planning of Wuxi and Jiangsu Province [grant number Z201610, H201656].

Compliance with ethical standards

All procedures performed in this study involving human participants were in accordance with the ethical standards of the institutional and/or national research committee and with the 1964 Helsinki declaration and its later amendments or comparable ethical standards. It was approved by the ethics committee of Jinling Hospital, People's Hospital of Hainan Province, and the Second Xiangya Hospital of Central South University. All participants provided written informed consent after a detailed description of this study.

Conflict of interest The authors declare that they have no conflicts of interest.

References

1. Benjet C, Bromet E, Karam EG, Kessler RC, McLaughlin KA, Ruscio AM, Shahly V, Stein DJ, Petukhova M, Hill E, Alonso J, Atwoli L, Bunting B, Bruffaerts R, Caldas-de-Almeida JM, de Girolamo G, Florescu S, Gureje O, Huang Y, Lepine JP, Kawakami N, Kovess-Masfety V, Medina-Mora ME, Navarro-Mateu F, Piazza M, Posada-Villa J, Scott KM, Shalev A, Slade T, ten Have M, Torres Y, Viana MC, Zarkov Z, Koenen KC (2016) The epidemiology of traumatic event exposure worldwide: results from the World Mental Health Survey Consortium. Psychol Med 46:327–343. https://doi.org/10.1017/S0033291715001981
2. Shalev A, Liberzon I, Marmar C (2017) Post-traumatic stress disorder. N Engl J Med 376:2459–2469. https://doi.org/10.1056/NEJMra1612499
3. American Psychiatric Association (2013) DSM-V, Diagnostic and statistical manual of mental disorders, 5th edn. American Psychiatric Inc, Arlington
4. Green JD, Annunziata A, Kleiman SE, Bovin Mj, Harwell AM, Fox AML et al (2017) Examining the diagnostic utility of the DSM-5 PTSD symptoms among male and female returning veterans. Depress Anxiety 34:752–760. https://doi.org/10.1002/da.2266
5. Menon V (2011) Large-scale brain networks and psychopathology: a unifying triple network model. Trends Cogn Sci 15:483–506. https://doi.org/10.1016/j.tics.2011.08.003
6. Enyuan Y, Zhengluan L, Yunfei T, Yaju Q, Zhu J, Han Z et al (2017) High-sensitive neuroimaging biomarkers for the identification of amnestic mild cognitive impairment based on resting-state fMRI and a triple network model. Brain Imaging Behav. https://doi.org/10.1007/s11682-017-9727-6
7. Biswal BB, Mennes M, Zuo XN, Gohel S, Kelly C, Smith SM et al (2017) Toward discovery science of human brain function. Proc Natl Acad Sci U S A 107:4734–4739. https://doi.org/10.1073/pnas.0911855107
8. Jovanovic T, Kazama A, Bachevalier J, Davis M (2012) Impaired safety signal learning may be a biomarker of PTSD. Neuropharmacology 62:695–704. https://doi.org/10.1016/j.neuropharm.2011.02.023
9. Sripada RK, King AP, Welsh RC, Garfinkel SN, Wang X, Sprpada CS et al (2012a) Neural dysregulation in posttraumatic stress disorder: evidence for disrupted equilibrium between salience and default mode brain networks. Psychosom Med 74:904–911. https://doi.org/10.1097/PSY.0b013e318273bf33
10. Koch SB, van Zuiden M, Nawijn L, Nawjin L, Frijling JL, Veltman DJ, Olff M (2016) Aberrant resting-state brain activity in posttraumatic stress disorder: a meta-analysis and systematic review. Depress Anxiety 33:592–605. https://doi.org/10.1002/da.22478
11. Patel R, Spreng RN, Shin LM, Girard TA (2012) Neurocircuitry models of posttraumatic stress disorder and beyond: a meta-analysis of functional neuroimaging studies. Neurosci Biobehav Rev 36:2130–2142. https://doi.org/10.1016/j.neubiorev.2012.06.003
12. Sheynin J, Liberzon I (2017) Circuit dysregulation and circuit-based treatments in posttraumatic stress disorder. Neurosci Lett 649:133–138. https://doi.org/10.1016/j.neulet.2016.11.014
13. Bluhm RL, Williamson PC, Osuch EA (2009) Alterations in default network connectivity in posttraumatic stress disorder related to early-life trauma. J Psychiatry Neurosci 34:187–194
14. Qin P, Northoff G (2011) How is our self related to midline regions and the default-mode network? NeuroImage 57:1221–1233. https://doi.org/10.1016/j.neuroimage.2011.05.028
15. Aupperle RL, Melrose AJ, Stein MB, Paulus MP (2012) Executive function and PTSD: disengaging from traums. Neuropharmacology 62:686–694. https://doi.org/10.1016/j.neuropharm.2011.02.008
16. St Jacques PL, Kragel PA, Rubin DC (2013) Neural networks supporting autobiographical memory retrieval in posttraumatic stress disorder. Cogn Affect Behav Neurosci 13:554–566. https://doi.org/10.3758/s13415-013-0157-7
17. Lanius RA, Frewen PA, Tursich M, Jetly R, Mckinnon MC (2015) Restoring large-scale brain networks in PTSD and related disorders: a proposal for neuroscientifically-informed treatment interventions. Eur J Psychotraumatol 6:27313. https://doi.org/10.3402/ejpt.v6.27313
18. Sripada RK, King AP, Garfinkel SN, Wang X, Sripada CS, Welsh RC (2012b) Altered resting-state amygdala functional connectivity in men with posttraumatic stress disorder. J Psychiatry Neurosci 37:241–249. https://doi.org/10.1503/jpn.110069
19. Rabinak CA, Angstadt M, Welsh RC, Kenndy AE, Lyubkin M, Martis B, Phan KL (2011) Altered amygdala resting-state functional connectivity in post-traumatic stress disorder. Front Psychiatry 2:62. https://doi.org/10.3389/fpsyt.2011.00062
20. Brown VM, LaBar KS, Haswell CC, Gold AL, Mid-Atlantic, Mirecc Workgroup, McCarthy G et al (2014) Altered resting-state functional connectivity of basolateral and centromedial amygdala complexes in posttraumatic stress disorder. Neuropsychopharmacology 39:351–359. https://doi.org/10.1038/npp.2013.197
21. Jin C, Qi R, Yin Y, Yin Y, Hu X, Duan L et al (2014) Abnormalities in whole-brain functional connectivity observed in treatment-naive post-traumatic stress disorder patients following an earthquake. Psychol Med 44:1927–1936. https://doi.org/10.1017/S003329171300250X
22. Zhu H, Qiu C, Meng Y, Cui H, Zhang Y, Huang X, Zhang J, Li T, Gong Q, Zhang W, Lui S (2015) Altered spontaneous neuronal activity in chronic posttraumatic stress disorder patients before and after a 12-week paroxetine treatment. J Affect Disord 174:257–264. https://doi.org/10.1016/j.jad.2014.11.053
23. Ke J, Chen F, Qi R, Xu Q, Zhong Y, Chen L, Li J, Zhang L, Lu G (2016) Post-traumatic stress influences local and remote functional connectivity: a resting-state functional magnetic resonance imaging study. Brain Imaging Behav 11:1316–1325. https://doi.org/10.1007/s11682-016-9622-6
24. Chen CC, Henson RN, Stephan KE, Kilner JM, Friston KJ (2009) Forward and backward connections in the brain: a DCM study of functional asymmetries. NeuroImage 45:453–462. https://doi.org/10.1016/j.neuroimage.2008.12.041
25. Friston KJ, Kahan J, Biswal B, Razi A (2014) A DCM for resting state fMRI. NeuroImage 94:396–407. https://doi.org/10.1016/j.neuroimage.2013.12.009
26. Udomratn P (2008) Mental health and the psychosocial consequences of natural disasters in Asia. Int Rev Psychiatry 20:441–444. https://doi.org/10.1080/09540260802397487
27. Weather F, Litz B, Herman D, Huska J, Keane T (1994) The PTSD Checklist-Civilian Version (PCL-C). National Center for PTSD, Boston
28. Weathers FW, Keane TM, Davidson JR (2001) Clinician-administered PTSD scale: a review of the first ten years of research. Depress Anxiety 13:132–156
29. First M, Spitzer R, Gibbons M, Williams J (1995) Structured clinical interview for DSM-IV. Biometrics Research Department. New York State Psychiatric Institute, New York
30. Weschler D (1987) WMS-R: Wechsler Memory Scale-Revised. Psychological Corporation, New York
31. Zung WW (1971) A rating instrument for anxiety disorders. Psychosomatics 12:371–379. https://doi.org/10.1016/S0033-3182(71)71479-0
32. Zung WW (1965) A self-rating depression scale. Arch Gen Psychiatry 12:63–70

33. Yan CG, Zhang YF (2010) DPARSF: a MATLAB toolbox for "pipeline" data analysis of resting-state fMRI. Front Syst Neurosci 4:13. https://doi.org/10.3389/fnsys.2010.00013
34. Calhoun VD, Adali T, Pearlson GD, Pekar JJ (2001) A method for making group inferences from functional MRI data using independent component analysis. Hum Brain Mapp 14:140–151
35. Shirer WR, Ryali S, Rykhlevskaia E, Menon V, Greicius MD (2012) Decoding subject-driven cognitive states with whole-brain connectivity patterns. Cereb Cortex 22:158–165. https://doi.org/10.1093/cercor/bhr099
36. Tsvetanov KA, Henson RN, Tyler LK, Tyler LK, Razi A, Geerligs L et al (2016) Extrinsic and intrinsic brain network connectivity maintains cognition across the lifespan despite accelerated decay of regional brain activation. J Neurosci 36:3115–3126. https://doi.org/10.1523/JNEUROSCI.2733-15.2016
37. Rosa MJ, Friston K, Penny W (2012) Post-hoc selection of dynamic causal models. J Neurosci Methods 208:66–78. https://doi.org/10.1016/j.jneumeth.2012.04.013
38. Crone JS, Schurz M, Holler Y, Bergmann J, Monti M, Schmid E et al (2015) Impaired consciousness is linked to changes in effective connectivity of the posterior cingulate cortex within the default mode network. NeuroImage 110:101–109
39. Friston KJ, Harrison L, Penny W (2003) Dynamic causal modelling. NeuroImage 19:466–477
40. Tu YK, Wu YC (2017) Using structural equation modeling for network meta-analysis. BMC Med Res Methodol 17:104. https://doi.org/10.1186/s12874-017-0390-9
41. Friston K (2011) Dynamic causal modeling and Granger causality comments on: the identification of interacting networks in the brain using fMRI: model selection, causality and deconvolution. NeuroImage 58:303–305. https://doi.org/10.1016/j.neuroimage.2009.09.031
42. Zhang Y, Xie B, Chen H, Li M, Liu F, Chen F (2016) Abnormal functional connectivity density in post-traumatic stress disorder. Brain Topogr 29:405–411. https://doi.org/10.1007/s10548-016-0472-8
43. Hutchinson JB, Uncapher MR, Wagner AD (2009) Posterior parietal cortex and episodic retrieval: convergent and divergent effects of attention and memory. Learn Mem 16:343–356. https://doi.org/10.1101/lm.919109
44. Moores KA, Clark CR, McFarlane AC, Brown GC, Puce A, Taylor DJ (2008) Abnormal recruitment of working memory updating networks during maintenance of trauma-neutral information in post-traumatic stress disorder. Psychiatry Res 163:156–170. https://doi.org/10.1016/j.pscychresns.2007.08.011
45. Fried PJ, Rushmore RJ, Moss MB, Valero-Cabre A, Pascual-Leone A (2014) Causal evidence supporting functional dissociation of verbal and spatial working memory in the human dorsolateral prefrontal cortex. Eur J Neurosci 39:1973–1981. https://doi.org/10.1111/ejn.12584
46. Scolari M, Seidl-Rathkopf KN, Kastner S (2015) Functions of the human frontoparietal attention network: evidence from neuroimaging. Curr Opin Behav Sci 1:32–39. https://doi.org/10.1016/j.cobeha.2014.08.003
47. White SF, Costanzo ME, Blair JR, Roy MJ (2015) PTSD symptom severity is associated with increased recruitment of top-down attentional control in a trauma-exposed sample. NeuroImage Clin 7:19–27. https://doi.org/10.1016/j.nicl.2014.11.012
48. Seeley WW, Menon V, Schatzberg AF, Keller J, Glover GH, Kenna H, Reiss AL, Greicius MD (2007) Dissociable intrinsic connectivity networks for salience processing and executive control. J Neurosci 27:2349–2356. https://doi.org/10.1523/JNEUROSCI.5587-06.2007
49. McTeague LM, Goodkind MS, Etkin A (2016) Transdiagnostic impairment of cognitive control in mental illness. J Psychiatr Res 83:37–46. https://doi.org/10.1016/j.jpsychires.2016.08.001
50. Shiba Y, Oikonomidis L, Sawiak S (2017) Converging prefronto-insula-amygdala pathways in negative emotion regulation in marmoset monkeys. Biol Psychiatry 17:31715–31718. https://doi.org/10.1016/j.biopsych.2017.06.016
51. Friston KJ, Mechelli A, Turner R, Price GJ (2000) Nonlinear responses in fMRI: the balloon model, Volterra kernels, and other hemodynamics. NeuroImage 12:466–477. https://doi.org/10.1006/nimg.2000.0630
52. Jun K, Li Z, Rongfeng Q, Qiang X, Yuan Z, Tao L, Jianjun L et al (2018) Typhoon-related post-traumatic stress disorder and trauma might lead to functional integration abnormalities in intra- and inter-resting state networks: a resting-state fMRI independent component analysis. Cell Physiol Biochem 48:99–110. https://doi.org/10.1159/000491666